NASA Technical Paper 2840

September 1988

Measurement of Local High-Level, Transient Surface Heat Flux

Curt H. Liebert

NASA

NASA Technical Paper 2840

1988

Measurement of Local High-Level, Transient Surface Heat Flux

Curt H. Liebert
Lewis Research Center
Cleveland, Ohio

National Aeronautics and Space Administration

Scientific and Technical Information Division

Summary

A method for simultaneously obtaining dual measurements of heat flux at the same surface location is presented. This work is part of a continuing investigation to develop methods for measuring local transient surface heat flux. The heat flux is obtained from transient temperature measurements taken at locations within a heat flux gage. These temperatures are used to measure (calculate) the surface heat fluxes corresponding to both the heat stored and the heat conducted within the gage. The gage was located at the gas-side surface of a rocket engine nozzle throat, and heat flux measurements were made during engine startup and into quasi-steady engine operation. At startup an increase in transient heat flux from about 4 MW/m^2 to 19 MW/m^2 was measured in 0.4 sec. During quasi-steady engine operation a decrease in heat flux from about 22 MW/m^2 to 10 MW/m^2 was measured in 0.6 sec. Possible applications of this method are for heat flux measurements on the turbine blade surfaces of space shuttle main engine turbopumps and on the component surfaces of rocket and advanced gas turbine engines and for testing sensors in heat flux gage calibrators.

Introduction

A method for measuring surface heat flux (heat transfer rate per unit area) was developed from both theoretical and experimental considerations. The application is for determining local, fast transient heat flux to turbine blades operating in space shuttle main engine (SSME) turbopumps. Thermal transients generated in the turbine blades are suspected to cause durability problems such as blade cracking (ref. 1). The effect of these thermal transients needs to be studied. Heat flux gages (sensors) are needed to obtain surface heat flux information for verifying analytical stress, boundary layer, and heat transfer design models used in engine component life prediction codes.

Some heat flux gages rely on extrapolating temperature and heat transfer information to a surface from points within a thermally conducting solid body. This method of determining heat flux is based on the inverse heat conduction problem (IHCP). IHCP has been studied and applied to dynamic and steady-state measurements for over 30 years. Past applications were related to missile nose cones, reentering heat shields, and rocket engine nozzles (refs. 2 to 4) and to thermal boundary layer studies on flat plates (ref. 5). These applications are especially difficult at transient heat transfer conditions. A major difficulty in applying IHCP is caused by uncertainties in obtaining heat flux values relative to random noise in measured temperature data. As is well known, variations of surface temperature will be attenuated at interior points. The resulting noise-to-signal ratios may be so large that it is impossible to predict meaningful heat flux values by extrapolating internal information to the surface. Many other shortcomings of IHCP are discussed in reference 2. In spite of the difficulties, many applications rely on IHCP because it is often not feasible to place sensors on surfaces exposed to hostile environments.

This study used IHCP techniques and thermoplug heat flux gages internally instrumented with thermocouples to determine if meaningful transient surface heat fluxes can be measured in a rocket engine nozzle throat during engine startup and into quasi-steady engine operation. The conditions simulated anticipated SSME startup and quasi-steady turbopump turbine conditions. Temperature information obtained with the gage was applied in a transient heat conduction equation to calculate surface heat flux. The temperature-variable physical properties of the thermoplug material—specific heat, thermal conductivity, and density—were considered. Property information was obtained from experimental values given in the literature (refs. 6 and 7). Least-squares equations were incorporated to define relevant property variations with temperature and also to express time and spatial variations of temperature and heat transfer quantities determined within the gage.

The results presented in this report include plots of (1) gas pressures measured in the rocket engine nozzle throat over a time interval including startup and operation into quasi-steady engine conditions, (2) transient temperatures measured at three locations on the thermoplug, and (3) measured transient surface heat fluxes. The factors believed to have contributed to the measurement uncertainty are listed.

Symbols

C_p	specific heat at constant pressure, J/kg K
k	thermal conductivity, W/m K
L	thermoplug length, m
$\mathbf{n}$	unit normal vector
$\dot{q}$	surface heat flux, W/m^2

r correlation coefficient

T absolute temperature, K

t sample time, sec

Z distance along axis of cylindrical body, m; thermocouple locations, m

ρ fluid density, kg/m^3

Subscripts:

c conducted

s stored

meas measured

Analysis

Figure 1 shows a schematic of a heat flux gage mounted in a wall. The gage body (thermoplug) is cylindrical, and one end or active surface is exposed to an external hot environment. The energy source may be generated by any means and can be in either a transient or steady-state condition. This external energy may be transferred to the active surface by convection and radiation heat transfer.

A major consideration in using heat flux gages is to make sure that they measure local surface heat flux. This can be accomplished by insulating the thermoplug on all surfaces except the active surface (fig. 1). Figure 2 shows a heat balance on a gage. The conventional one-dimensional heat conduction equation expressing these conditions is

$$\rho C_p \frac{\partial T}{\partial t} = \frac{\partial}{\partial Z}\left(k \frac{\partial T}{\partial Z}\right), \text{ W/m}^3 \qquad (1)$$

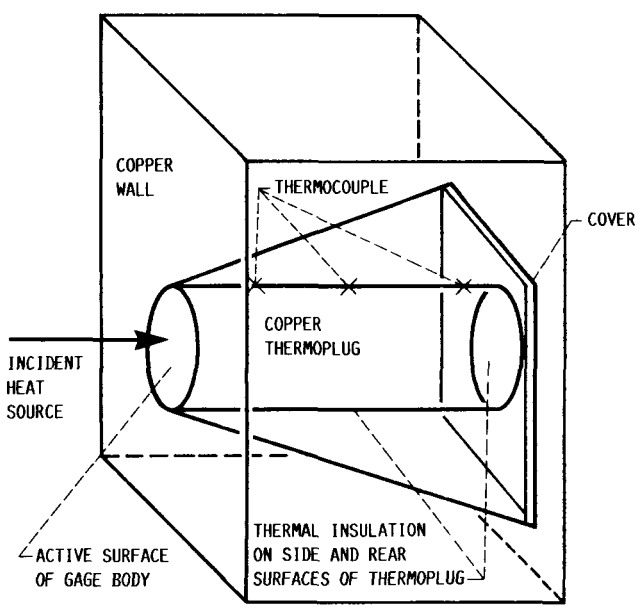

Figure 1.—Heat flux gage mounted in wall.

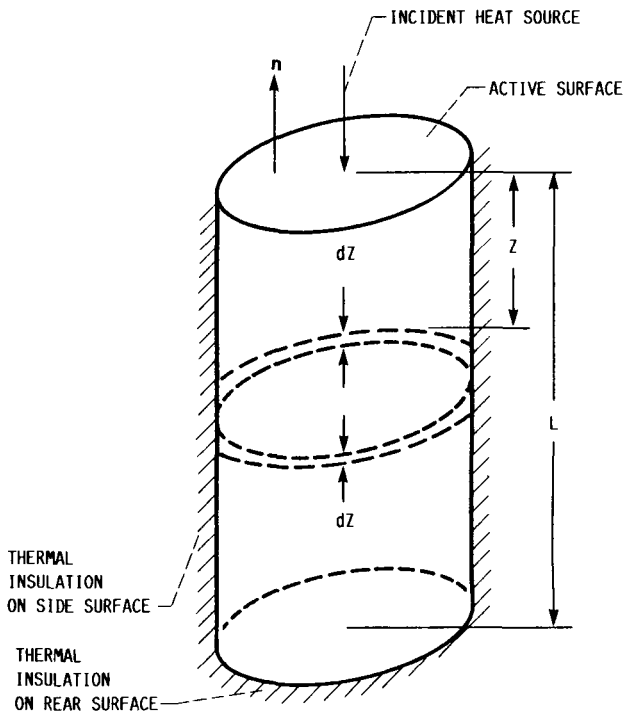

Figure 2.—Heat balance on thermoplug.

The term on the left side of equation (1) is the local heat transfer rate per unit volume stored within the thermoplug. The term on the right side is the local heat transfer rate per unit volume conducted within the thermoplug. For the purposes of this investigation, each side of equation (1) is treated separately. Integrating over the thermoplug length leads to the following heat flux expressions for the left and right sides of equation (1):

$$\dot{q}_s = \int_0^L \left(\rho C_p \frac{\partial T}{\partial t}\right) dZ, \text{ W/m}^2 \qquad (2)$$

and

$$\dot{q}_c = \int_0^L \frac{\partial}{\partial Z}\left(k \frac{\partial T}{\partial Z}\right) dZ, \text{ W/m}^2 \qquad (3)$$

Evaluating equation (3) yields

$$\dot{q}_c = k \frac{\partial T}{\partial Z}\bigg|_{Z=0} \qquad (4)$$

since $k(\partial T/\partial Z) = 0$ at $Z = L$. Equations (2) and (3) express dual time-dependent conservation of one-dimensional heat flux.

The two separate quantities, $\dot{q}_s$ and $\dot{q}_c$, are related in different ways to the temperature field. One way is through the density, specific heat, and temperature history. The other

way is through the thermal conductivity and the temperature gradient. Closely matched values of $\dot{q}_s$ and $\dot{q}_c$ add credence to the heat flux measurement method. Because both $\dot{q}_s$ and $\dot{q}_c$ are considered, this is called a dual heat flux measurement.

Calculation Method

The method for calculating dual transient surface heat flux with equations (2) and (3) by using curve-fit equations to describe variations of pertinent variables is illustrated in this section. The curve-fit criterion used in this sample calculation was that the equations should fit the data within a deviation of ± 1 percent with corresponding correlation coefficients r of 0.999 or larger. The curve fits describe straight-line, parabolic, and exponential equations. When the heat fluxes have been determined, the heat conduction equation (eq.(1)) has been solved.

Sample Calculation of $\dot{q}_s$

The term under the integral sign in equation (2) is expressed as $\rho C_p(\partial T/\partial t)$. This term was evaluated at thermocouple location $Z = 0.508$ cm and at sample time $t = 0.9$ sec. The temperature of the thermoplug at the specified time and location was measured as 367 K (fig. 3(b)). From this temperature, the thermal properties C_p and ρ could then be found from figures 4(a) and (b). Next, $\partial T/\partial t$ was evaluated. To do this, thermoplug temperature data (figs. 3(b) and 5) measured at $Z = 0.508$ cm and at three times, say $t = 0.8$, 0.9, and 1.0 sec, were used to form a parabolic least-squares, curve-fit (fig. 5) equation expressing temperature as a function of time. Note that the time range includes the specified time ($t = 0.9$ sec). This least-squares equation was differentiated to obtain an equation for the partial derivative of temperature with respect to time. The value of $\partial T/\partial t$ was calculated by substituting $t = 0.9$ sec into this equation. Multiplying the values found for the two thermal properties by the partial derivative resulted in a value of 1270 MW/m^3 for the heat transfer rate per unit volume at $Z = 0.508$ cm and $t = 0.9$ sec. This value is plotted in figure 6.

Only a limited number (three) of time values were used to develop the temperature history curve-fit equation for determining $\partial T/\partial t$ because the curve changes from concave to convex at approximately 0.9 sec. At other times considered in this study, curve fits could be accomplished over longer time increments with more than three time values because there were no concave-to-convex irregularities in the curves.

Calculations for $\rho C_p(\partial T/\partial t)$ were repeated with equation (2) at $Z = 0.902$ and 1.778 cm. The values for $\rho C_p(\partial T/\partial t)$ at these locations were computed at 780 and 282 MW/m^3 and are plotted in figure 6. A two-parameter exponential least-squares, curve-fit equation was formed for the three values of $\rho C_p(\partial T/\partial t)$ calculated at the three specified Z values. The area under the exponential least-squares curve is equal to the stored surface heat flux value (eq. (2)). This

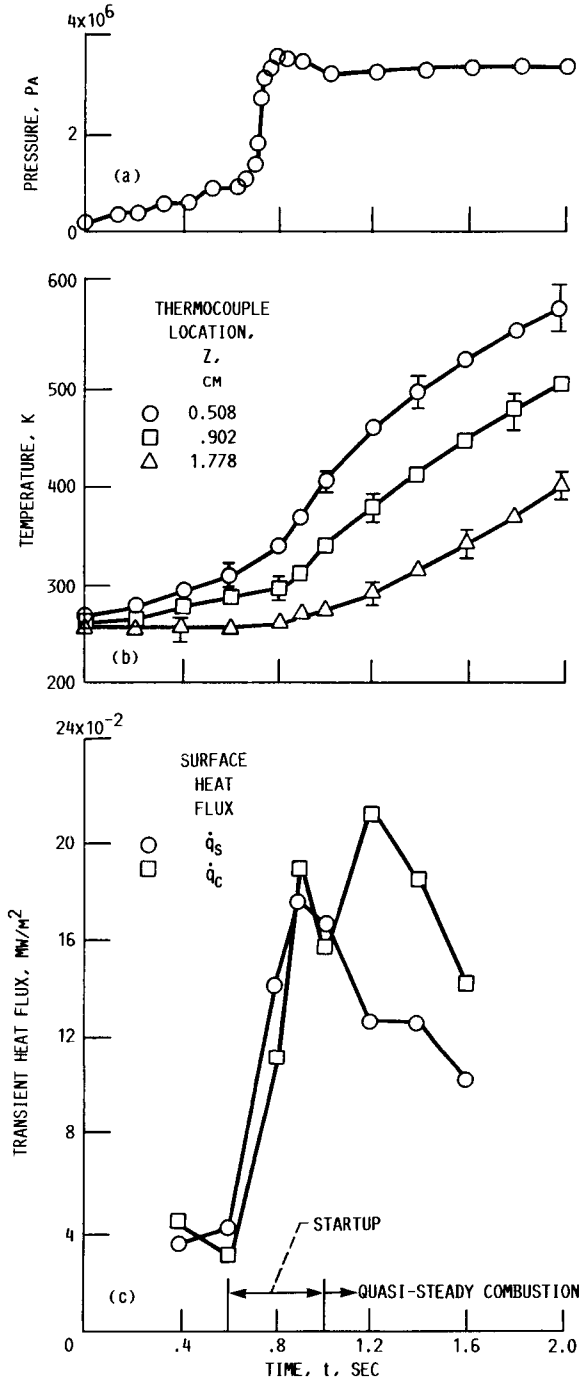

(a) Combustion gas pressure.
(b) Measured thermoplug temperature. Recovery temperature, 2080 K.
(c) Surface heat flux history.

Figure 3.—Measured combustion gas pressure, thermoplug temperature, and surface heat flux.

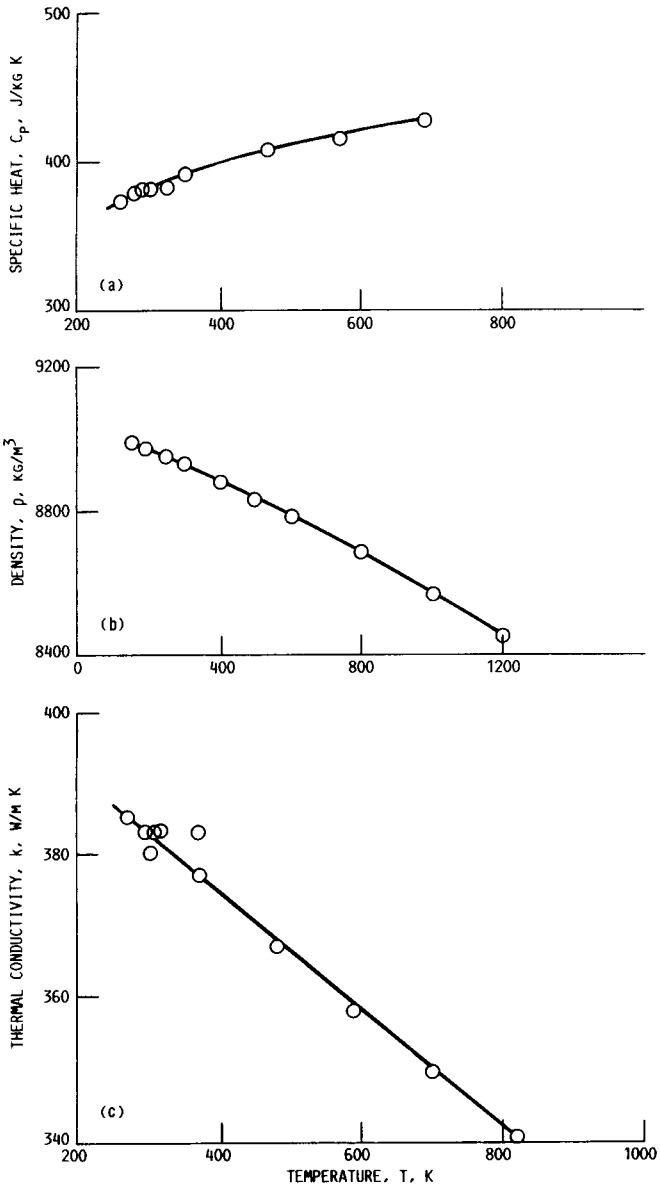

(a) Specific heat. Experimental error, ±0 to 10 percent.
(b) Density. Experimental error, ±0 to 1 percent.
(c) Thermal conductivity. Experimental error, ±0 to 10 percent.

Figure 4.—Physical properties of copper thermoplug as function of temperature.

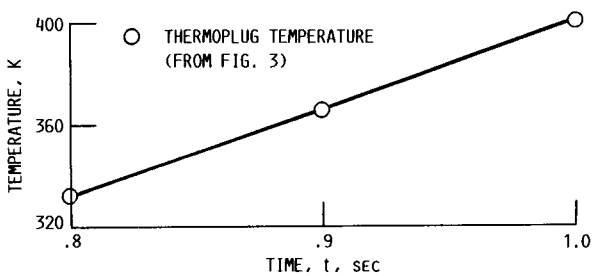

Figure 5.—Parabolic least-squares curve fit of temperature history at thermocouple location $Z = 0.508$ cm and sample time $t = 0.9$ sec. Correlation coefficient $r = 0.999$.

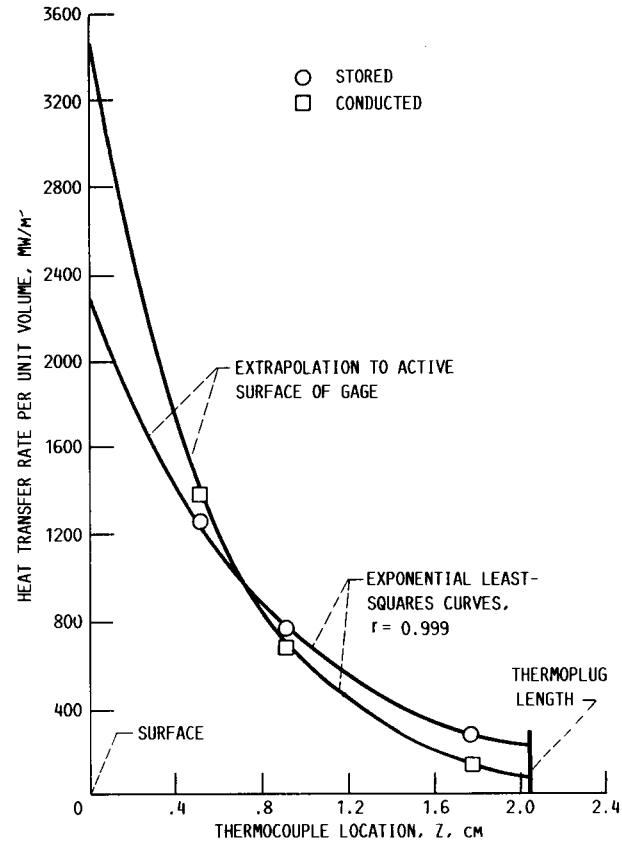

Figure 6.—Heat transfer rate per unit volume as function of thermocouple location. Sample time $t = 0.9$ sec.

equation was integrated over the thermoplug length to give $\dot{q}_s = 17.5$ MW/m^2.

Sample Calculation of $\dot{q}_c$

Values of $k(\partial T/\partial Z)$ were evaluated at $Z = 0.508$, 0.902, and 1.778 cm for $t = 0.9$ sec. (Values for k are shown in fig. 4(c).) Then a least-squares, exponential, curve-fit equation expressing the values of $k(\partial T/\partial Z)$ as a function of temperature measurement location was obtained. This equation was evaluated at $Z = 0$ to give $\dot{q}_c = 19.19$ MW/m^2 (eq. (4)). Values of the associated heat transfer rate conducted per unit volume $\partial[k(\partial T/\partial Z]/\partial Z$ (eq. (3)) were also calculated and are shown in figure 6 for comparison with stored values.

Another method for determining $\dot{q}_c$ at the surface is to evaluate the heat transfer rate per unit volume at each thermocouple location, curve fit these data (fig. 6), and then integrate the curve-fit equation over the thermoplug length. This procedure is equivalent to that for calculating $\dot{q}_s$. Both methods for determining $\dot{q}_c$ numerically agreed.

Apparatus and Experimental Procedures

The following discussion summarizes the apparatus and experimental procedure descriptions in references 3 and 4. The

rocket nozzle (fig. 7) was fabricated from pure copper. The thermoplug was also fabricated from pure copper because references 3, 4, and 8 demonstrate the necessity for fabricating thermoplugs from material identical to those of the wall within which they are mounted. The use of the same materials minimizes the intrusiveness of the gage within its environment.

Figure 7 schematically shows how a thermoplug was installed in the copper throat wall of a rocket nozzle. A tapered hole was machined through the wall at the throat region. The hole was tapered to allow space for inserting thermal insulation around the thermoplug. The uninsulated end of the thermoplug, formed from a right-circular cylinder, was pressed into the smallest diameter of the tapered hole. The smallest diameter was located at the gas-side surface. The uninsulated end of the cylinder, machined to the nozzle throat contour, formed the active surface of the gage. This active surface was in direct contact with the hot combustion gases. An aluminum oxide cement was placed in the gap between the thermoplug and the wall. The aluminum oxide cement was used to minimize heat conduction between the gases. An aluminum oxide cement was placed in the gap between the thermoplug and the wall. The aluminum oxide cement was used to minimize heat conduction between the thermoplug and the metal walls of the nozzle. The thermoplug was held in place by a cover fastened to the nozzle outside surface. The cover was insulated from the thermoplug. The side and rear surfaces of the thermoplug were polished to minimize radiation exchange between these surfaces and the insulation. Chromel-Alumel wire thermocouples were mounted onto the thermoplug. The thermocouple hot junction diameters were about 0.040 cm. The positions of the thermocouples on a thermoplug are shown in figure 7.

The rocket engine was operated during startup and into quasi-steady engine operation on a thrust stand. Nozzle throat gas pressures were recorded with an oscillograph. Thermoplug transient temperature data obtained with the thermocouples were also recorded with an oscillograph.

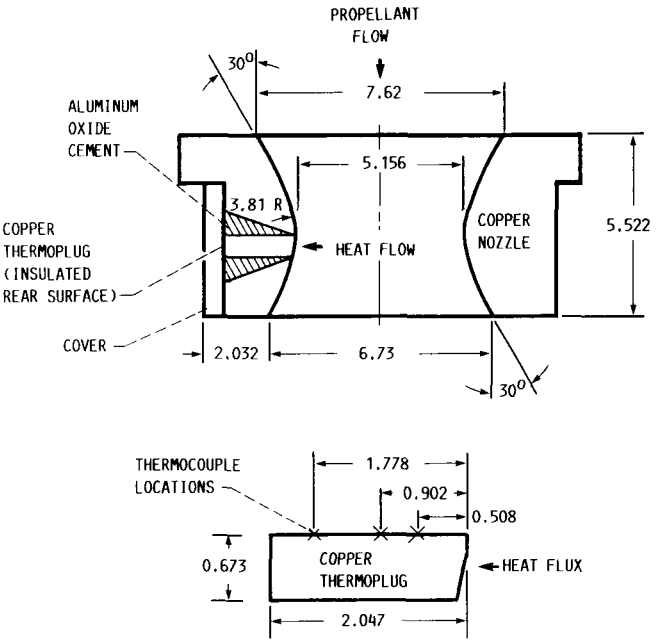

Figure 7.—Installation of thermoplug in nozzle throat. (Dimensions are in centimeters.)

Results and Discussion

Measured Heat Flux

Combustion gas pressures, thermoplug temperatures, and heat fluxes measured on the rocket engine throat surface during startup and into quasi-steady combustion conditions are shown in figure 3. The measured heat flux values are comparable to those anticipated in uncooled turbines driving SSME turbopumps, in advanced rocket and gas turbine engines, and in heat flux sensor calibrators (ref. 9).

During engine startup, when gas pressure (fig. 3(a)) and thermoplug temperature (fig. 3(b)) were rising rapidly with time, the surface heat flux (fig. 3(c)) rapidly increased from about 4 MW/m^2 to 19 MW/m^2 in about 0.4 sec. Then, during quasi-steady operation, when the gas pressure was nearly steady, the heat flux decreased less rapidly from about 22 MW/m^2 to 10 MW/m^2 in 0.6 sec. Agreement of $\dot{q}_c$ and q_s was better during startup transient conditions than at quasi-steady conditions.

These trends of transient surface heat flux measured during engine startup and into quasi-steady engine operation are reasonable. During startup the measured gas-side heat flux should rise rapidly as the heat released by the combustion process and the heat transfer coefficient both increase rapidly with time. At the quasi-steady hot gas conditions after startup, internal gage temperatures and therefore gage surface temperatures increased at a slower rate toward the recovery temperature of 2080 K. By Newton's law of cooling, measured surface heat flux at quasi-steady pressure conditions is expected to decrease because the difference between the relatively constant gas temperature and the increasing surface temperature becomes less while heat transfer coefficients remain reasonably constant.

Heat Flux Measurement Uncertainty

Ideally, $\dot{q}_s = \dot{q}_c$; but figure 3(c) shows that these values were not equal in this investigation. The following factors could contribute to the divergence in stored and conducted heat fluxes:

(1) Data-recording system
(2) Thermal gradients along thermocouple hot junction and thermocouple wires
(3) Experimental error associated with thermal property measurements
(4) Curve fitting of
  (a) Temperature history
  (b) Temperature gradient
  (c) Thermal properties

(5) Unwanted heat leaks to or from wall
(6) Gage intrusiveness due to
    (a) Hole in wall filled with insulation
    (b) New boundary-layer temperature distribution setup
(7) Restrictions on number of temperature measurements that can be made on small gages

The uncertainty associated with many of these factors is unknown.

One very important uncertainty is associated with curve fits of the heat transfer rates per unit volume shown in figure 6. Evaluating this uncertainty is very difficult because these values must be extrapolated to the active surface of the thermoplug (fig. 6). Obviously the magnitude of the dual heat fluxes could have been determined more accurately if thermocouples could have been located nearer the active surface of the gage as well as nearer the gage rear surface.

An arc lamp source was used to compare surface heat fluxes obtained with thermoplug flux gages and those measured with commercial factory gages. This was done in a heat flux gage calibration facility at the Lewis Research Center (ref. 9). Preliminary results show that the heat flux values agree to ± 20 percent. These comparisons were made at heat flux levels of approximately 4 to 6 MW/m^2.

Concluding Remarks

The method proposed herein for measuring (calculating) local, high-level transient surface heat flux is feasible. Important factors in understanding the characteristics of the method, which is based on the inverse heat conduction problem, are the influence of the properties and pure mathematical parameters associated with the heat transfer model and the approximate nature of the physical model and the heat flux calculation method. Study of these factors led to the conclusions that the consideration of temperature-variable physical properties can be important and that more credence can be given to a heat flux calculation method when thermocouples are placed very close to the active and rear surfaces of the gage.

References

1. Liebert, C.H.: Heat Flux Sensor Calibrator. Structural Integrity and Durability of Reusable Space Propulsion Systems, NASA CP-2381, 1985, pp. 195–198.
2. Beck, J.V.; Blackwell, B.; and St. Clair, C.R., Jr.: Inverse Heat Conduction. Ill-Posed Problems. John Wiley and Sons, 1985.
3. Liebert, C.H.; Hatch, J.E.; and Grant, R.W.: Application of Various Techniques for Determining Local Heat-Transfer Coefficients in a Rocket Engine From Transient Experimental Data. NASA TN D-277, 1960.
4. Liebert, C.H.; and Ehlers, R.C.: Determination of Local Experimental Heat-Transfer Coefficients of Combustion Side of an Ammonia-Oxygen Rocket. NASA TN D-1048, 1961.
5. Liebert, C.H., et al.: High-Temperature Thermocouple and Heat Flux Gage Using a Unique Thin Film—Hardware Hot Junction. J. Engr. Gas Turbines Power, vol. 107, no. 4, Oct. 1985, pp. 938–944.
6. Touloukian, Y.S., et al.: Thermophysical Properties of Matter. Vol.1—Thermal Conductivity, Metallic Elements, and Alloys. IFI/Plenum, New York, 1970.
7. Rohsenow, W.M.; Hartnett, J.P.; and Ganic, E.N.: Handbook of Heat Transfer Fundamentals. McGraw-Hill, 1985.
8. Westkaemper, J.C.: On the Error in Plug-Type Calorimeters Caused by Surface-Temperature Mismatch. J. Aerospace Sci., vol. 28, no. 11, Nov. 1961, pp. 907–908.
9. Liebert, C.H.: Heat Flux Calibration Facility Capable of SSME Conditions. Structural Integrity and Durability of Reusable Space Propulsion Systems, NASA CP-2471, 1987, pp. 47–49.

NASA
National Aeronautics and Space Administration

Report Documentation Page

1. Report No.	2. Government Accession No.	3. Recipient's Catalog No.
NASA TP-2840		

4. Title and Subtitle	5. Report Date
Measurement of Local High-Level, Transient Surface Heat Flux	September 1988
	6. Performing Organization Code

7. Author(s)	8. Performing Organization Report No.
Curt H. Liebert	E-4200
	10. Work Unit No.
	582-01-11

9. Performing Organization Name and Address	11. Contract or Grant No.
National Aeronautics and Space Administration Lewis Research Center Cleveland, Ohio 44135-3191	
	13. Type of Report and Period Covered
12. Sponsoring Agency Name and Address	Technical Paper
National Aeronautics and Space Administration Washington, D.C. 20546-0001	14. Sponsoring Agency Code

15. Supplementary Notes

16. Abstract

This study is part of a continuing investigation to develop methods for measuring local transient surface heat flux. A method is presented for simultaneous measurements of dual heat fluxes at a surface location by considering the heat flux as a separate function of heat stored and heat conducted within a heat flux gage. Surface heat flux information is obtained from transient temperature measurements taken at points within the gage. Heat flux was determined over a range of 4 to 22 MW/m^2. It was concluded that the method is feasible. Possible applications are for heat flux measurements on the turbine blade surfaces of space shuttle main engine turbopumps and on the component surfaces of rocket and advanced gas turbine engines and for testing sensors in heat flux gage calibrators.

17. Key Words (Suggested by Author(s))	18. Distribution Statement
Instrumentation Heat flux	Unclassified – Unlimited Subject Category 35

19. Security Classif. (of this report)	20. Security Classif. (of this page)	21. No of pages	22. Price*
Unclassified	Unclassified	9	A02

NASA FORM 1626 OCT 86

*For sale by the National Technical Information Service, Springfield, Virginia 22161

NASA-Langley, 1988